Physical and Dynamical Ingredients Required for the Development of Above-Anvil Cirrus Plumes

Joel D. McAuliffe
National Weather Center Research Experiences for Undergraduates, Norman, Oklahoma
East Carolina University Department of Geography, Greenville, North Carolina

Cameron R. Homeyer
School of Meteorology, University of Oklahoma, Norman, Oklahoma

ABSTRACT

The formation of above-anvil cirrus plumes atop deep convection is an important contributor to water vapor transfer from the troposphere to the lower stratosphere. It has been observed that these plume features have been associated with severe weather activity. However, the factors contributing to the development of these cirrus plumes are unknown. Here we show that the main ingredients required for this process are directional wind shear between cell motion and upper level detrainment and penetration of the tropopause using a combination of geostationary satellite imagery, high-resolution three-dimensional radar observations, and radiosonde observations. Temperature and vertical wind speed shear do not show consistent characteristics for environments conducive to the development of above-anvil cirrus. Some plume cases show fluctuations in cloud top heat signatures when analyzed with infrared satellite imagery, indicating mixing of the plume into the lower stratosphere. Our results demonstrate how environmental and physical characteristics affect plume formation and support assertions in previous studies on the relevance of above-anvil cirrus plumes for increases in stratospheric water vapor content, which is relevant to predictions of future climate. We also present a relationship between hail occurrence and overshooting top depth that may result in an increase in lead time for warnings of severe storms.

1. INTRODUCTION

Severe storms have the ability to create features significant for advancing our understanding of meteorology and climate. One such feature is the formation of protruding, dome-shaped tops above the anvil of deep convection, which can be an indicator of storm severity (Dworak et al., 2012). Another feature is the above-anvil cirrus plume, which forms in the wake of a descending overshooting top of a convective tower (Fujita, 1982). Several studies have observed these cirrus plumes from satellites in both visible and infrared bands, and from aircraft with visible imagery and polarization lidar (Fujita 1982; Adler et al. 1983; Mack et al. 1983; Sphinhire et al. 1983; Stevák and Doswell 1991; Levizzani and Setvák 1996). Questions remain on how these clouds form. An overshooting top can extend into the lower stratosphere, but is it required for convection to reach these altitudes for the above-anvil cirrus to form? Previous studies have argued that above-anvil cirrus plumes represent injection of cloud particles into the lower stratosphere, based largely on infrared temperatures warmer than the tropopause coincident with some plume cases (Adler et al. 1981; Fujita, 1982; Negri 1982; Mack et al. 1983; Homeyer 2014).

Once a storm overshoots the tropopause, gravity wave breaking and additional turbulent processes lead to irreversible mixing (injection) of cloud particles and tropospheric air into the lower stratosphere. Wang (2003, 2004) shows that a breaking gravity wave along and above the anvil can result in the development of these plumes. The dome shape of the overshooting top directly

influences wind speed and direction: inside the domes will you find vertical winds reaching speeds around 40 m s^{-1} whereas outside the dome you will find slower winds with high directional shear (Wang, 2005), which can lead to localized wave breaking.

In past studies, these above-anvil cirrus were known as an indicator of severe weather. During the 2012 SRSOR period, it was determined that 57% of plume-producing storms were severe and 85% of plumes appeared before a severe weather report, averaging out to a lead time of 18 min (Bedka et. al, 2015). These storm systems also produced large hail. In addition to above-anvil plumes in visible imager, previous studies have linked the related warm cloud top signatures from IR to severe weather including hail and tornadoes (McCann 1983; Adler et al. 1985; Brunner et al. 2007).

In addition to their association with severe weather, above-anvil cirrus plumes may have significant chemistry and climate impacts related to the injection of water vapor into the lower stratosphere. In particular, stratospheric water vapor injection can lead to an alteration of the chemical form of chlorine in the lower stratosphere, such that the inorganic chlorine shifts to the catalytically active free radical form (ClO). The polar regions have observed ozone depletion due to this chemical reaction, which lead to the formation of the infamous ozone hole in the Southern Hemisphere (Solomon et al. 1986).

The temperature at which activation of the chlorine radical begins is sensitive to the amount stratospheric water vapor. Large increases in water vapor concentration from convective injection allows for ozone destruction at warmer stratospheric temperatures than in Polar Regions, which makes chlorine-driven ozone destruction a global chemistry and climate problem (Anderson et al., 2012). In addition, water vapor itself is a greenhouse gas and contributes significantly to Earth's radiation budget, particularly in the upper troposphere and lower stratosphere. Stratospheric water vapor content is directly affected by transport through the tropopause region (Forster et al. 1998; Solomon et al. 2010). Though higher stratospheric water vapor has an overall cooling effect on the stratosphere, it has a reverse effect on the troposphere (Ackerman, 1988).

In this study, we seek to determine what atmospheric conditions and storm characteristics are conducive to the formation of above-anvil cirrus plumes. In order to accomplish this goal, a combination of high-resolution radiosonde observations, radar observations, and geostationary satellite imagery are collectively analyzed for a total of 15 independent cases. Section 2 describes the datasets and methods used, Section 3 presents the results of our analysis, and Section 4 summarizes our findings and discusses the results in the context of prior and future work.

2. Data and Methods

GOES data

In order to identify above-anvil cirrus plumes and their thermal characteristics, we use visible and Infrared (IR) imagery from the National Oceanic and Atmospheric Administration (NOAA) Geostationary Operational Environmental Satellite (GOES) system (Menzel and Purdom, 1994). In particular, above-anvil cirrus plumes are identified subjectively (i.e., by the human eye) in the visible imagery by looking for shadowing atop each storm and its proximity to overshooting. Figure 1a and 1b show examples of the GOES IR and visible imagery for one of the above-anvil cirrus plume cases identified in this study.

Visible and IR satellite imagery are obtained from two operational satellites: GOES-West and GOES-East. The nominal horizontal resolution for the imagery in the IR band is 4 km. For the visible band, the nominal horizontal resolution is 1 km. The temporal resolution ranges from 1-min to 15-min.

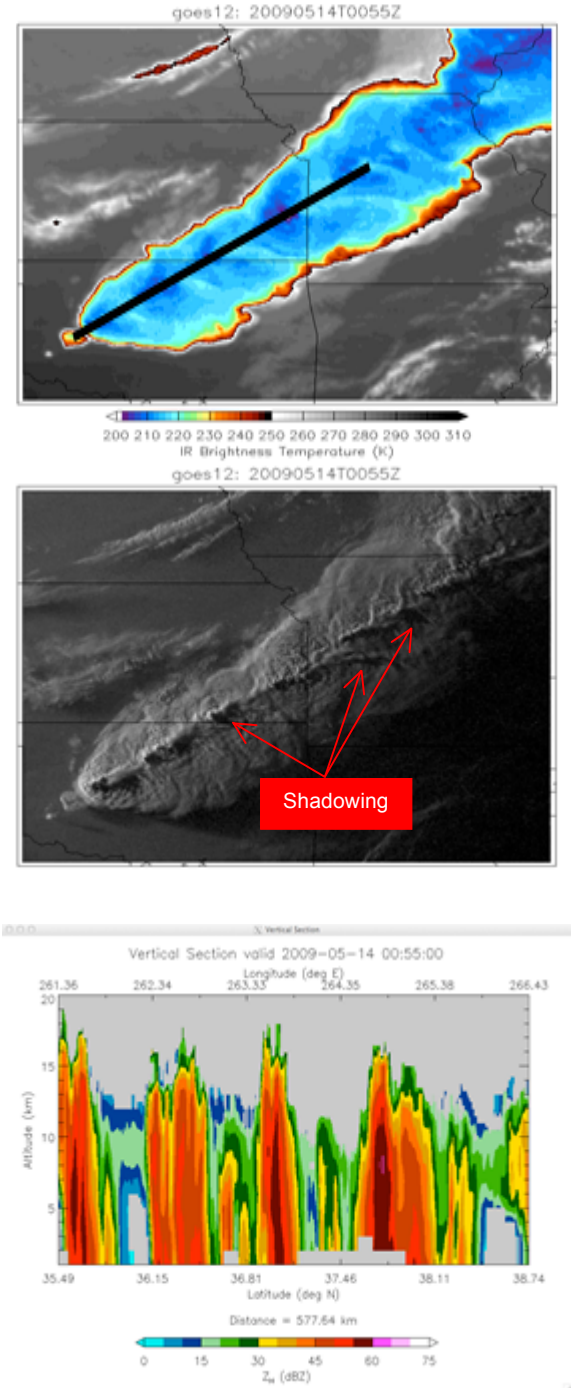

Figure 1: For a select time during the 14 May 2009 case: (a) GOES IR imagery, (b) GOES visible imagery, and (c) a vertical cross-section of the NEXRAD composite along the path (thick black line) in (a).

NEXRAD WSR-88D data

The Next Generation Weather Radar (NEXRAD) program Weather Surveillance Radar-1988 (WSR-88D) network consists of more than 150 dual-polarization S-band (10-cm wavelength) radars in the continental United States, providing nearly complete horizontal and vertical coverage of deep convection (Crum and Alberty, 1993). Data for individual radars is available at the National Climatic Data Center (NCDC). These radar systems operate 24 hours a day, with scans in predesignated, 360° sequences at different elevation angles. The resolution of the data is dependent on time, function, meteorological target, and the spherical range from the radar. Figure 1c is an example of the NEXRAD 3D output from the vertical cross-section drawn across the cloud top on Figure 1a. Variables considered when analyzing these deep convective storms include differential reflectivity Z_{DR}, specific differential phase K_{DP}, and the radar reflectivity factor at horizontal polarization Z_H. The polarimetric variables K_{DP} and Z_{DR} provide information on the shape of hydrometeors. Further information on the polarimetric variables can be found in several textbooks and journal articles (e.g., Doviak and Zrnić 1993; Bringi and Chandrasekar 2001).

For analysis, we merge data from individual systems into high-resolution, three-dimensional composites following the methods of Homeyer (2014) and Homeyer and Kumjian (2015). In particular, each volume scan is merged onto a common Cartesian grid using a combination of interpolation and averaging. The resolution of the radar composites is 0.02° longitude-latitude (~2 km) in the horizontal dimension and 1 km in the vertical dimension, with composites for each case made at 5-minute intervals.

Radiosonde data

Radiosonde data is from operational launches by National Weather Service (NWS)

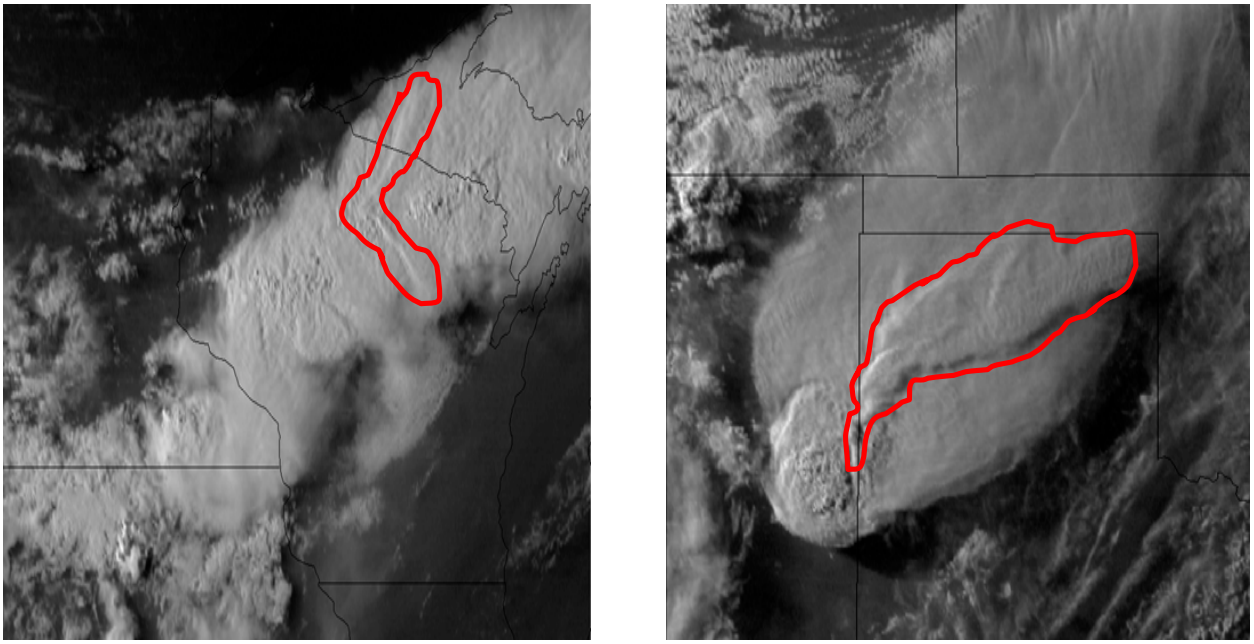

Figure 2: GOES visible imagery examples of the two above-anvil cirrus plumes identified in this study: (LEFT) a wispy plume on 21 Aug 2013 and (RIGHT) a rigid plume on 8 May 2010.

forecast offices in the continental US, which take place daily at 0000 and 1200 UTC. Data from 0000 UTC only is used in this study, since all cases coincide with this observational time. Data is obtained from sites in close proximity to the location of the each storm in order to evaluate the most representative conditions of its environment.

Analysis Methods

For analysis, 10 cases of above-anvil plumes were identified using GOES visible imagery. These cases occurred during a span of 5 years (2009 to 2014). The locations of these events were heavily concentrated in central United States: Colorado, Texas, Oklahoma, Kansas, Arkansas, and Missouri. One case was located in Michigan.

Above-anvil cirrus plume cases were individually examined with the NEXRAD radar composites to determine the physical characteristics of each storm including their depth and tropopause-relative altitude. In particular, subjective analysis of vertical cross-sections that bisect the overshooting top and above-anvil cirrus plumes was the primary method used. Z_H was used to help determine storm severity and particle size, while K_{DP} and Z_{DR} were primarily used to identify hail signatures. These radar observations were analyzed along with NWS Storm Prediction Center severe weather reports to determine their relationship with hail occurrence at the surface. The radiosonde data were used to identify the tropopause altitude and determine the characteristics of each storms environment.

3. Results and Discussion

As outlined in the Introduction, it is not clear based on previous studies whether or not a storm must penetrate the tropopause to produce an above-anvil cirrus plume. In order to improve upon this limited understanding, the depth of each storm was evaluated in each case using the NEXRAD radar observations. These data demonstrate that storms in each case extend into the lower stratosphere, confirming that above-anvil cirrus plumes likely represent stratospheric injection of cloud particles. The minimum-recorded storm height above the tropopause

was about 0.6 km whereas the maximum height was about 6.2 km. Table 1 summarizes these findings for all above-anvil cirrus plume cases.

In addition to their association with tropopause-penetrating convection, we found two distinct textural characteristics for above-anvil plumes in the GOES visible imagery: wispy (or diffuse) and rigid (or textured). Figure 2a shows an example of a wispy cirrus plume. In the cases investigated here, wispy cirrus plumes often forked downstream of the overshooting top, producing two above-anvil cirrus plumes. Figure 2b shows an example of a rigid plume. These were often found to expand rapidly over time and capable of extending over half of the broader convective anvil. These textural differences appeared to be associated with the depth of overshooting, where wispy plumes were common in cases with higher overshooting depths and rigid plumes were more common in cases with lower overshooting depths.

As mentioned previously, there is no current explanation for what factors contribute to the development of cirrus plumes. In order to examine the role of environmental factors in the development of above-anvil plumes in more detail, we evaluate profiles of temperature and wind speed at relative altitudes to the tropopause from radiosonde observations near each storm. Figure 3 shows three of these profiles for above-anvil cirrus plume cases. As Figure 3 demonstrates, we find no consistent relationship between plume development and the temperature structure or wind speed shear above the tropopause.

Despite no consistent relationship between tropopause-relative temperature and wind speed, further examination of producing cases revealed a clear and consistent environmental characteristic. Namely, storms that produced above-anvil plumes were found to show significant misalignment in the direction of storm motion and upper level detrainment (i.e., anvil direction). Furthermore, similar analysis of 5 additional cases of tropopause-penetrating convection where no plumes were observed in GOES imagery showed the opposite behavior (i.e., alignment of storm motion and upper-level detrainment). Table 1 summarizes these findings for cases with and without above-anvil cirrus plumes.

Severe weather events were observed in every case with an above-anvil cirrus plume. In particular, each case produced large hail, with a minimum report of 1 inch in diameter. We examined storm characteristics in the

DATE	PEAK ALTITUDE (km)	TROPOPAUSE (km)	T-R DEPTH (km)	PLUME PRODUCING (Y/N)	ANVIL DIRECTION	CELL DIRECTION
5/13/2009	19	12.8	6.2	Y	ENE	SSW
*6/7/2009 (A)	17	13.3	3.7	Y	ENE	N
*6/7/2009 (B)	18	13.3	4.7	Y	NNE	ESE
*6/7/2009 (C)	15	14.4	0.6	Y	NE	ENE
*6/7/2009 (D)	17	13.6	3.4	N	ENE	ENE
6/8/2010	17	15.5	1.5	Y	NE	SW
6/13/2010	18	16.4	1.6	Y	N	ENE
4/8/2011	16	11.2	4.8	Y	ENE	N
5/17/2013	19	12.9	6.1	Y	E	W
*5/18/2013 (A)	13	11.2	1.8	N	NNE	NNE
*5/18/2013 (B)	16	11.3	4.7	N	NE	NE
5/20/2013	18	14	4	N	NE	NE
*5/28/2013 (A)	19	12.8	6.2	Y	NE	SW
*5/28/2013 (B)	17	11.8	5.2	Y	E	N
5/31/2013	19	14	5	N	NE	NE
6/27/2013	19	15.1	3.9	N	SE	SE
8/21/2013	17	12.8	4.2	Y	SE/ENE	ENE/SE
5/20/2014	16	12.5	3.5	Y	NE	SE
6/5/2014	15	12.9	2.1	Y	ENE	SSW

Table 1: This table represents data obtained for each case. Columns from left to right: date of plume-producing event, peak overshooting top altitude, level of tropopause, tropopause-relative depth, whether or not the system produced a plume, anvil detrainment direction, and convection cell direction of propagation.

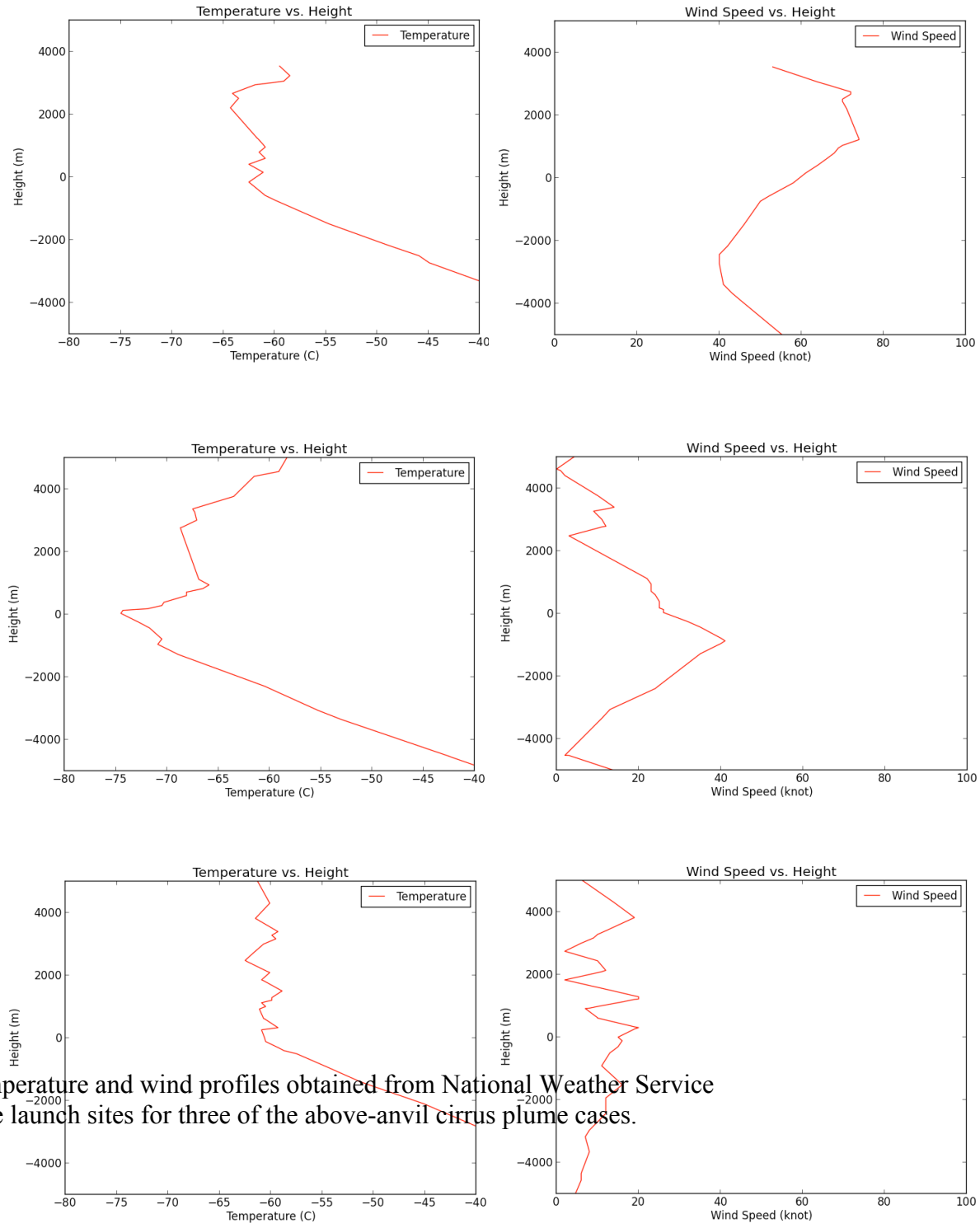

Fig. 3 Temperature and wind profiles obtained from National Weather Service Radiosonde launch sites for three of the above-anvil cirrus plume cases.

radar observations prior to and during each hail event to determine any clear relationships between the radar observables and hail production. Based on detailed analysis of 8 storms, we found a consistent relationship between overshooting top evolution and hail occurrence. In particular, the overshooting top was found to increase in altitude over time, before leveling off or decreasing in altitude between 5 and 15 minutes before hail occurrence. Some of the storm systems produced tornadoes; however, there is no direct relationship between overshooting tops or above-anvil cirrus plumes and tornado formation.

4. Summary and Discussion

Based on detailed analysis of 10 above-anvil cirrus plume cases and 5 cases without above-anvil plumes, we have found that tropopause-relative temperature structure and wind speed are not directly related to above-anvil cirrus plume formation. On the other hand, a difference in the direction of storm motion and upper level detrainment was found to be essential. If the storm propagates in a different direction than the detraining anvil cloud, a plume will form. If a storm propagates in the same direction as the detraining anvil, plume formation is unlikely. In addition, all above-anvil cirrus plume cases were associated with convection overshooting the tropopause altitude. Depths of stratospheric penetration ranged from 0.6 to 6.2 km, with the depth of overshooting largely associated with two distinct textural appearances: wispy or rigid. In particular, deeper storms were associated with wispy plumes and shallower storms were associated with rigid plumes. In addition, it was found that above-anvil cirrus plumes and overshooting top evolution may be useful predictors for large hail.

The formation of above-anvil cirrus plumes has been linked with troposphere-to-stratosphere transport of water vapor. The findings in this study support this linkage, which provides a positive feedback between intensifying convection and global warming. Increased concentrations of stratospheric water vapor are known to decrease stratospheric temperatures and increase tropospheric temperatures (Solomon et al., 2010). Furthermore, increases in stratospheric water vapor from deep convection have been argued to activate chemical reactions leading to a rapid depletion of ozone. Thus, further examination of these storms with more cases and alternative datasets (such as those including chemistry) is needed to improve our understanding of their climate impacts.

Future work is also needed to examine the relationships between tropopause-penetrating convection and above-anvil cirrus plumes in more detail. If the findings in this study from a limited set of cases hold, there is significant potential for improved warnings related to increased lead time, which ultimately saves lives and protects properties. The importance and processes leading to the formation of the two textural appearances of above-anvil plumes found in this study is also a topic of future work.

5. Acknowledgements

The research within this paper has been funded by the National Science Foundation under grant AGS 1062932 and operated under the National Weather Center Research Experience for Undergraduates program. This program was monitored under Dr. Daphne LaDue. The authors thanks Andrew Dzambo for assistance with Python scripting and providing comments that helped improve the paper.

6. References

Ackerman, T. P., K. Liou, L Pfister, and F. P. J. Valero, 1988: Heating rates in tropical anvils. *J. Atmos. Sci.,* **45**, 1606-1623. doi: http://dx.doi.org/10.1175/1520-0469(1988)045<1606:HRITA>2.0.CO;2

Adler, R. F., D. D. Fenn, and D. A. Moore, 1981: Spiral feature observed at top of rotating thunderstorm. *Mon. Wea. Rev.*, **109**, 1124-1129.

Adler, R. F., Markus, D. D. Fenn, G. Szejwach, and W. E. Shenk, 1983: Thunderstorm top structure observed by aircraft overflights with an infrared radiometer. *J. Climate Appl. Meteor.*, **22**, 579-593

Adler, R. F., Markus, and D. D. Fenn, 1985: Detection of severe midwest thunderstorms using geosynchronous satellite data. *Mon. Wea. Rev.*, **113**, 769-781.

Anderson, J. G., D. S. Sayres, J. B. Smith, and D. M. Wilmouth, 2012: UV dosage levels in summer: increased risk of ozone loss from convectively injected water vapor. *Science*, **337**, 835-839.

Bedka, K. M., L. D. Carey, W. Feltz, J. Kanak, R. Rogers, and C. Wang, 2015: Examining deep convective cloud evolution using total lightning, WSR-88D, and GOES-14 super rapid scan datasets. *Wea. Forecasting*, **30**, 571-590. doi: http://dx.doi.org/10.1175/WAF-D-14-00062.1

Bringi, V. N., and V. Chandrasekar, 2001: *Polarimetric Doppler Weather Radar.* Cambridge University Press, 636 pp.

Brunner, J. C., S. A. Ackerman, A. S. Bachmeier, and R. M. Rabin, 2007: A quantitative analysis of the enhanced-V feature in relation to severe weather. *Wea. Forecasting*, **22**, 853-872.

Corti, T., Q. Fu, B. P. Luo, T. Peter, and H. Vömel, 2006: The impact of cirrus clouds on tropical troposphere-to-stratosphere transport. *Atmos. Chem. Phys.*,**6**, 2539-2547.

Crum, T. D., and R. L. Alberty, 1993: The WSR-88D and the WSR-88D operational support facility. *Bull. Amer. Meteor. Soc*., **74**, 1669-1687.

Doviak, R. J., and D. S. Zrnić, 1993: *Doppler Radar and Weather Observations.* 2nd ed. Dover Publications, 592 pp.

Dworak, R., K. M. Bedka, J. Brunner, and W. Feltz, 2012: Comparison between GOES-12 overshooting top detections, WSR-88D radar reflectivity, and severe storm reports. *Wea. Forecasting*, **27**, 684-699. doi:10.1175/WAF-D-11-00070.1.

Forster, P. M. D., and K. P. Shine, 1999: Stratospheric water vapour changes as a possible contributor to observed stratospheric cooling. *Geophys. Res. Lett.*, **26**, 3309-3312

Fujita, T. T., 1982: Principle of stereoscopic height computations and their applications to stratospheric cirrus over severe thunderstorms. *J. Meteor. Soc. Japan*, **60**, 355-368.

Homeyer, C. R., 2014: Formation of the enhanced-V infrared cloud-top feature from high-resolution three-dimensional radar observations. *J. Atmos. Science,* **71**, 332-348. doi: http://dx.doi.org/10.1175/JAS-D-13-079.1

Homeyer, C. R., and M. R. Kumjian, 2015: Microphysical characteristics of overshooting convection from polarimetric radar observations. *J. Atmos. Science,* **72**, 870-891. doi: http://dx.doi.org/10.1175/JAS-D-13-0388.1

Levizzani, V., and M. Setvák, 1996: Multispectral, high-resolution satellite observations of plumes on top of convective storms. *J. Atmos. Sci.*, **53**, 361-369.

Mack, R. A., A. F. Hasler, and R. F. Adler, 1983: Thunderstorm cloud-top observations using satellite stereoscopy. *Mon. Wea. Rev.*, **111**, 1949-1964.

McCann, D. W., 1983: The enhanced-V: A satellite observable severe storm signature. *Mon. Wea. Rev.*, **111**, 887-894.

Menzel, W. P., and J. F. W. Purdom, 1994: Introducing GOES-I: The first of a new generation of geostationary operational environmental satellites. *Bull. Amer. Meteor. Soc.,* **75**, 757-781. doi: http://dx.doi.org/10.1175/1520-0477(1994)075<0757:IGITFO>2.0.CO;2

Negri, A. J., 1982: Cloud-top structure of tornadic storms on 10 April 1979 from rapid scan and stereo satellite observations. *Bull. Amer. Soc.*, **63**, 1151-1159.

Solomon, S., R. R. Garcia, F. S. Rowland, and D. J. Wuebbles, 1986: On the depletion of Antarctic ozone. *Nature*, **321**, 755-758.

Solomon, S., K. H. Rosenlof, R. W. Portmann, J. S. Daniel, S. M. Davis, T. J. Sanford, and G. Plattner, 2010: Contributions of stratospheric water vapor to decadal changes in the rate of global warming. *Science*, **327**, 1219-1223.

Spinhirne, J. D., M. Z. Hansen, and J. Simpson, 1983: The structure and phase of cloud tops as observed by polarization lidar. *J. Climate Appl. Meteor.*, **22**, 1319-1331.

Setvák, M., and C. A. Doswell, 1991: The AVHRR channel-3 cloud-top reflectivity of convective storms. *Mon. Wea. Ref.*, **119**, 841-847.

Wang, P. K., 2003: Moisture plumes above thunderstorm anvils and their contributions to

cross tropopause transport of water vapor in midlatitudes. *J Geophys. Res.*, **108** (D6), 4194. doi:10.1029/2003JD002581.

Wang, P. K., 2004: A cloud model interpretation of jumping cirrus above storm top. *Geophys. Res. Lett.*, **31**, L18106, doi:10.1029/2004GL020787

Wang, P. K., 2005: The thermodynamic structure atop a penetrating convective thunderstorm.*J. Atmos. Res.*, **83**, 254-262. doi:10.1016/j.atmosres.2005.08.010